A Stochastic $SIRV$ model to estimate the effective reproductive number for measles epidemic in Niger

Method Articles:

Abstract

Aims/ objectives: Cyclic recurrence of measles epidemics in developing countries induced high mortality, especially among malnourished children. In Niger, as the disease exhibits clearly seasonal outbreaks, we observe increasing incidence during the dry season, from October to June. In this article, we perform an inference on reported cases during 2017-2018 measles outbreak to yield effective reproductive number,R_p, for each of the eight administrative regions in Niger. Our method is based on the stochastic model SIR with vaccination of measles, relying on the Metropolis-Hastings algorithm as an analysis tool. The choice of this model takes into account the random fluctuations inherent to the epidemiological characteristics of rural populations of Niger, notably a high prevalence of measles in children under 5 years, coupled with very low immunization coverage. It follows from this analysis that some regions of Niger remained potentially vulnerable to measles outbreaks due to a very high R_p value in these regions, As evidenced by our simulation of epidemic trends in these regions, this is the case of the regions of Tahoua and Zinder. However, the low birth rate had sheltered certain regions from measles outbreaks, such as the Diffa and Dosso regions. We have indeed noted two dominant factors that explain the high values of R_p in these eight regions, the low vaccination coverage and the high birth rate. Mathematical models allow a better understanding of the dynamics of disease spread in a population. However, difficulty in data collection processes and estimation of statistics parameters limit their range in statistical analysis of epidemic spread. Other hand the numerical resolution takes a long time computationally.

Keywords: Measles; Compartmental model; Basic reproductive number; Markov chains; Monte

Carlo Methods; Stochastic simulation; Niger.
2010 Mathematics Subject Classification: *; *; *

1 Introduction

Measles is a highly contagious infectious disease caused by a morbillivirus, measles virus. Once a person has become infected, no specific antiviral treatment is available [1]. Transmission is mainly by direct contact with mouth or nasal secretions. Complications are more likely in children under 5 years and adults over 20 years [2, 3].

In developing countries, like Niger, measles remains one of the main causes of infant mortality because children under 5 years remain the most affected, summing up to 90% of deaths for this age group [4, 5, 2, 6]. In sub-Saharan Africa, and even more in areas where vaccination coverage is not optimal, the case fatality is one of the highest, reaching $5 - 10\%$, compared to that of high-income countries, where we have 1 death in this age group out of 1000 measles cases [7, 8, 9].

A fundamental concept that has come out of the measles transmission process is that of the basic reproduction number R_0. It is defined as average number of secondary infections produced when one infected individual is introduced into a host population where everyone is susceptible [10, 11]. It is well-known that R_0 is a threshold parameter in the course of the spread of measles disease. In fact, if $R_0 < 1$, the disease will eventually disappear from the population, while if $R_0 > 1$ the disease can spread as an epidemic in the absence of health interventions.

In a partially immunized population, the effective reproduction number R_p is the analogue of the basic reproduction number R_0, where p is the proportion of newborns vaccinated, and exhibits the contribution of vaccination in the control of an epidemic. In fact if $R_p > 1$, the minimum proportion of the susceptible population that must be vaccinated to prevent an epidemic is $1 - 1/R_p$, called the critical vaccination coverage of newborns [12].

In this wake, we estimate the effective reproductive number of 2018 measles outbreaks for each region using the Metropolis-Hasting Algorithm (MHA) and biweekly recorded measles cases. However, it is very difficult to forge a suitable statistical link between measles times series and a mathematical model, because only one state variable, the number of infected individuals, is observable. Moreover, it appears that in most situation, this variable is under-reported.

Section 2 is devoted to our materials and methods, we start by summarizing data related to characteristics of measles in Niger, following by our $SVIR$ model, which describes the stochastic dynamics of the disease. Then, we end this section with our analysis tools relying heavily on the Metropolis-Hastings algorithm. In section 3, we present the results of inference and some numerical simulations. Hence, we compare biweekly reported cases data to means of theirs analogues simulated from the estimated parameters. Our results should start a discussion and could aid the stakeholders to design strategic vaccination coverage for each region in Niger. Concluding remarks and direction for future research are provided in section 4.

2 Materials and Methods

2.1 Measles facts in Niger

Niger's population annual growth rate is 3.9%, as resulted from the last National population census hold in 2012. Henceforth, in 2018, the population of Niger amounted to $21,561,121$ with 4.32% allocated for infants under 1 year, 19.73% under 5 years and children under 15 years cumulate up to 51.18%.

Cases of measles have been obtained from the national compulsory notification disease database (Maladies à Déclaration Obligatoire – MDO Niger). Figure 1 is a sample of measles cases obtained from MDO Niger database [4].

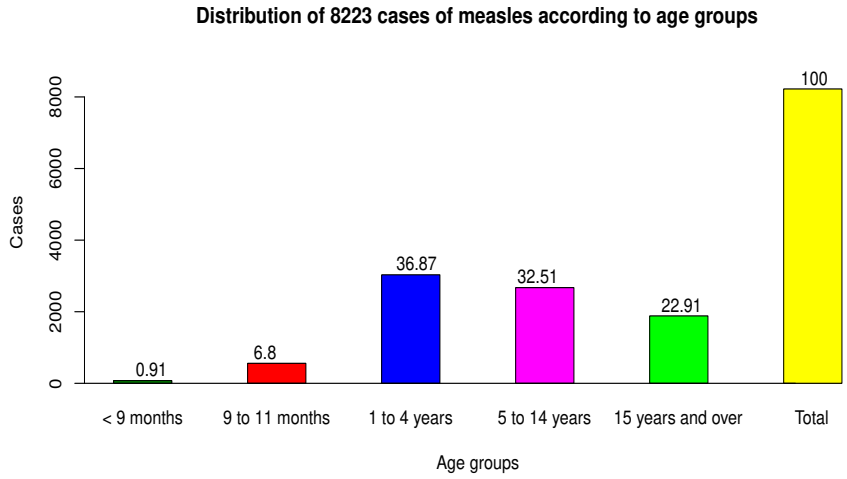

Figure 1: A sample of measles cases, between $0-5$ years range

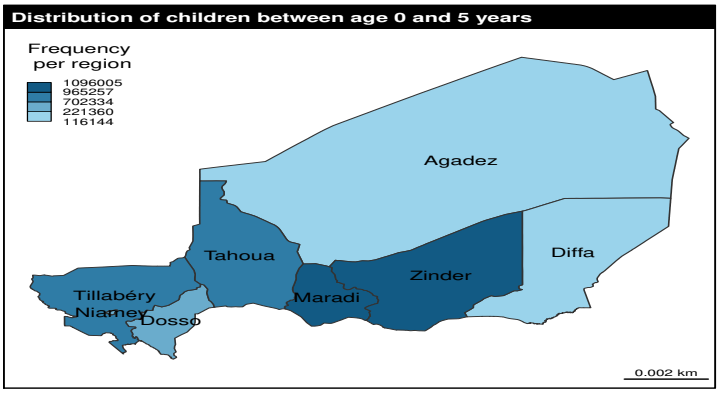

Figure 2: Age group $0-5$ years. Population projection $2012-2035$.

For the elimination of measles, in addition to national measles routine vaccination, Niger has planned Supplementary Vaccination Activities (AVS) against measles from 2012 to 2020 in all health districts. The primary vaccination is one dose administered in children between 9 and 11 months. Measles vaccine is 95% effective for preventing the disease just after one dose [2].

Measles is endemic in urban areas and remains frequent in areas where vaccination coverage is low. Age-dependent attack rate (AR) is likely to be higher in susceptible children less than 12

Region	<= 5years	$\delta = 5q_0$	< 1year	VC
Agadez	116144	$0,046$	21094	54%
Diffa	143583	$0,093$	26125	59%
Dosso	59299	$0,133$	111486	71%
Maradi	1075694	$0,114$	200921	61%
Niamey	247285	$0,056$	43630	35%
Tahoua	928445	$0,072$	169026	64%
Tillabery	807368	$0,141$	151208	61%
Zinder	1096005	$0,093$	207477	80%

Table 1: Measles vaccination coverage (VC) in children between $0-5$ years database: DSRE/PEV NIGER 2018

months of age. Table 1 shows measles VC in children between $0-5$ years [4] and child mortality risk ($\delta = 5q_0$), defined as risk of death before 5 years [13]. Figure 2 gives a repartition per region of children in the $0-5$ years range, the shading intensity reflects the importance of frequency.

According to MSF(Médecin Sans Frontière), to prevent the spread of measles, the protection of the population must reach a minimum of 95%. Such coverage rate is difficult to maintain among this population where a large part has transhumance livelihood with little access to the vaccination, usually available in urban health centers [14]. . By the way, there exists a batch of such infrastructures where the vaccination coverage rate does not even go beyond 50% (MSF). Figure 4 represents measles cases reported from 2011 to 2018 and figure 3 show measles cases per region recorded in 2018 as well as vaccination coverage, represented by ray discs proportional to vaccination coverage [15].

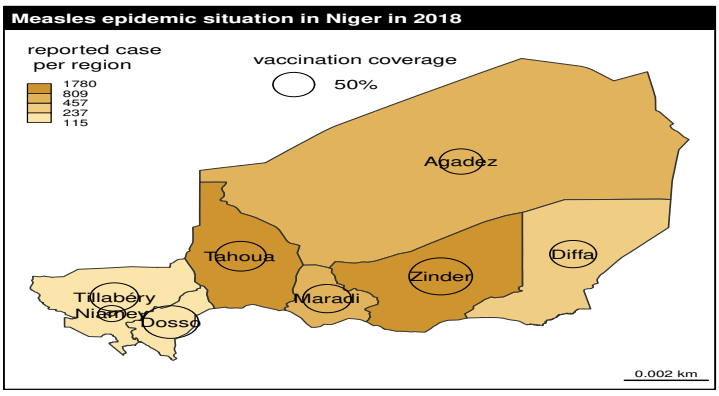

Figure 3: Vaccination coverage(VC), circles areas give the VC magnitude

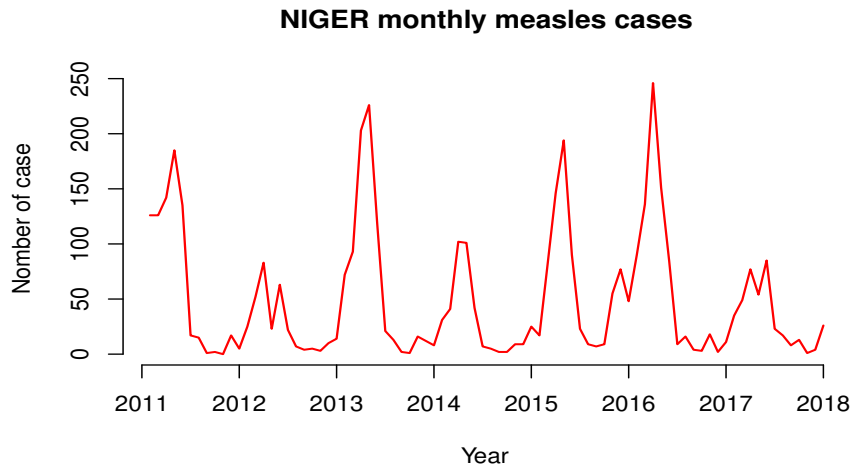

Figure 4: Database: DSRE/MDO-Niger

In a small, isolated population, measles epidemic cannot persist [16, 17, 18], Indeed, the spread of the disease subsides at term, due to a progressive immunization of a growing proportion of the population. Thus, in such a context, measles can only be endemic after regular importation of the virus, generally from infected migrants from large urban centers [19].

2.2 Mathematical model

In what follows, $S(t), I(t), R(t)$ denote respectively the number of susceptible, infected and immunized (susceptible vaccinated and recovered patients) at time t.

In this model, the new susceptible are introduced at a constant rate n. A fraction, pn, of newborns has acquired immunity by vaccination, the other fraction $(1-p)n$ remains susceptible. We assume that:

- the natural death rate is δ for each compartment.
- infectious individuals recover at the rate of γ.
- infectious individuals have an additional μ death rate from measles.
- we consider the standard incidence $f(I,S) = \beta SI$, β is the disease transmission coefficient. β is the average probability of an adequate contact between an infected and a susceptible per unit of time.

Under these assumptions we have [20, 21]:

$$R_p = \frac{(1-p)n\beta}{\delta(\mu+\gamma+\delta)} \tag{2.1}$$

In addition, $X_t = (S(t), I(t))_{t\geq 0}$ is a continuous-time homogeneous Markov chain on the denumerable state space $\mathbb{N}^2 = \{0, 1, 2, \cdots\}^2$. First, we assume that Δt can be chosen sufficiently small such that at most one change in state occurs during the time interval Δt. In particular, there

can be either a new infection, a birth, a death or a recovery. From of state $\{X_t = (s,i)\}$, only the following states are accessible:

$$(s,i);(s+1,i);(s,i-1);(s-1,i);(s-1,i+1).$$

corresponding to the possible transitions starting from the state (s,i). X_t has an absorbing set corresponding to disease-free equilibrium states $E_0 = \{(s,i), s \geq 0; i = 0\}$. Let $V_{(s,i)}$ be the set of neighbors of state (s,i):

$$V_{(s,i)} = \{(s+1,i);(s-1,i+1);(s-1,i);(s,i-1)\}$$

Setting $\tau_{(s,i)} = n(1-p) + \beta is + \delta s + (\mu + \delta + \gamma)i$, the transition probabilities of $X_t = (S(t), I(t))$, are defined by

$\mathbb{P}(\Delta X_t = (h,k)/X_t = (s,i)) =$

$$\begin{cases} n(1-p)\Delta t + o(\Delta t) & \text{if} \quad (h,k) = (1,0) \\ \beta si\Delta t + o(\Delta t) & \text{if} \quad (h,k) = (-1,1) \\ \delta s\Delta t + o(\Delta t) & \text{if} \quad (h,k) = (-1,0) \\ (\mu + \delta + \gamma)i\Delta t + o(\Delta t) & \text{if} \quad (h,k) = (0,-1) \\ 1 - \tau_{(s,i)}\Delta t + o(\Delta t) & \text{if} \quad (h,k) = (0,0), \end{cases} \tag{2.2}$$

where $\Delta X_t = X_{t+\Delta t} - X_t$ and those R_t process are defined by:

$\mathbb{P}(R_t = l/X_t = (s,i), R_t = r) =$

$$\begin{cases} \gamma i\Delta t + o(\Delta t) & \text{if} \quad l = 1 \\ \delta r\Delta t + o(\Delta t) & \text{if} \quad l = -1 \\ 1 - (i\gamma + \delta r)\Delta t + o(\Delta t) & \text{if} \quad l = 0 \end{cases} \tag{2.3}$$

In stochastic $SVIR$ model, the process $X_t = (S_t, I_t)$ is a Markov chain resulting from a set of transient states $\mathbb{N}^2 - E_0$, which evolves until it escapes to a set of absorbing states corresponding to disease-free equilibrium.

When the process reaches the set of absorbing states, it remains there permanently. However, before the instant of absorption, which is relatively long, the process passes through a quasi-stationary state. Under some conditions on R_p, the quasi-stationary distribution of the number of infected exists and can be closely approximated by geometric distribution [20, 21].

2.3 Usage of Metropolis-Hastings algorithm

Let $\theta = (I_0, \beta, \mu, \gamma, S_0, \delta, n, p) = (\theta_m, \theta_e)$ be the vector of model parameters where $\theta_e = (S_0, \delta, n, p)$ is the vector of parameters relative to the environment and $\theta_m = (I_0, \beta, \mu, \gamma)$ is the vector of parameters related to the disease. I_0 and S_0 are respectively the number of infected and susceptible at time 0. Let the sequence of the number of infected individuals, $(C_k)_{1 \leq k \leq N}$ in the time interval $]k-1, k]$: $C_k = \sum_{j=1}^{N_k} \mathbb{I}_{\{\Delta I_{t_j} = 1\}}$, where N_k is the jump number of $(I_t)_{t \geq 0}$ in the interval $]k-1, k]$. Then the series $(c_k^*)_{1 \leq k \leq N}$ is a partial observation of $(C_k)_{1 \leq k \leq N}$, that is, if $(c_k)_{1 \leq k \leq N}$ is a realization of $(C_k)_{1 \leq k \leq N}$ then for all $\quad 1 \leq k \leq N, \quad c_k = \rho c_k^*$

Similarly $(D_k)_{1\leq k\leq N}$ for the observations $(d_k^*)_{0\leq k\leq N}$. The parameter $\rho(k)=\rho$ depends on the environment, it is supposed to be constant during the observation period.

The objective is to estimate the vector θ_m for a value of θ_e fixed, given time series of reported cases $(c_k^*)_{0\leq k\leq N}$ and reported deaths $(d_k^*)_{0\leq k\leq N}$ observed. Recall that p is the proportion of newborns vaccinated. Let VE be the vaccine efficacy, we estimated p of $p=VE\times VC$. We assumed $VE=95\%$.

The unit of time is two weeks, corresponding to exposed and infectious period of measles[22]. In this case θ is the vector of the values of these parameters per unit time. The series $(c_k^*)_{0\leq k\leq N}$ is reported at a rate ρ and c_k^* is the number of individuals infected during the period $]k-1,k]$ and we count during the same period d_k^* deaths.

Figure 5 shows a sample path of (I_t) for Parameters values: $S_0=100$; $I_0=2$; $\beta=0.69$; $\delta=0.25$; $\mu=0.02$; $\gamma=0.14$; $n=3.33$; $p=0.40$; $t\in[0\quad 26]$; $k\in\{1,\cdots,26\}$. $R_p=13,44995$. In Figure 6, we have biweekly cases of (I_t).

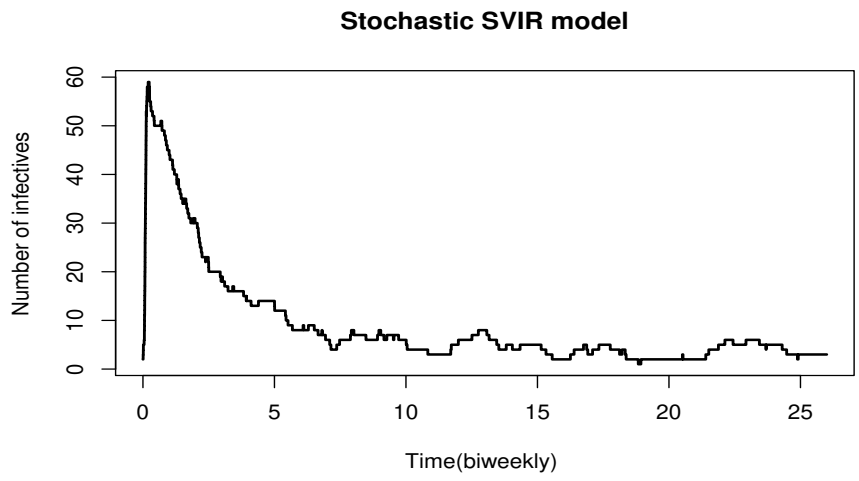

Figure 5: a sample path of (I_t)

Let $L(I,S,C,D,\theta_m/c^*,d^*,\theta_e)$ be the joint conditional distribution of the unobservable process and unknown parameters θ_m,, given the observable process and known parameters θ_e, we may write:

$$\begin{aligned} &L(I,S,C,D,\theta_m/c^*,d^*,\theta_e)= \\ &\mathbb{P}\left(\{I_k,S_k\},\{C_k,D_k\},0\leq k\leq N,\theta_m/\{c_k^*\},\{d_k^*\},\theta_e\right). \end{aligned} \tag{2.4}$$

Setting

$$L^*(.)=L(./\{c^*,d^*,\theta_e\}),$$

the problem reduces to the study of $L^*(\{C,D,\theta_m\})$. But it is necessary to find the relation between $\{I_{k+1},S_{k+1}\}$ and $\{I_k,S_k,C_k,D_k\}$ beforehand, in other words find a solution to the problem of the following filter by looking for the correct transfer functions H_1 and H_2 in the diagram figure 7.

$I_k=H_1(C_k,D_k,I_{k-1},S_{k-1},\theta,\varepsilon)$ et

$S_k=H_2(C_k,D_k,I_{k-1},S_{k-1},\theta,\varepsilon)$,

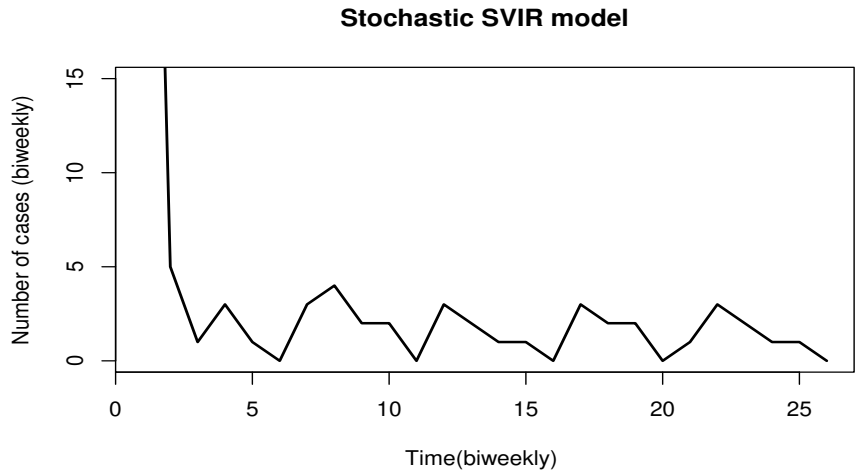

Figure 6: $C(k)$: biweekly cases of (I_t)

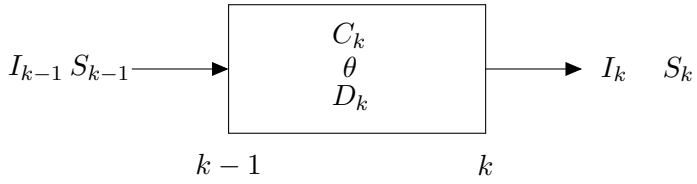

Figure 7: Model Filter

where ε is a random variable, I_k and S_k are respectively the numbers of infectious and susceptible at the end of the period $]k-1, k]$.

It follows from model assumptions the following relationships, for all $k, 1 \leq k \leq N$

$$\begin{aligned} S_k &= (1-\delta)(S_{k-1} + n(1-p) - C_k) \\ I_k &= (1-\gamma)(1-\delta)(C_k - D_k) \end{aligned} \tag{2.5}$$

Then we may write now the joint posterior distribution :

$$L^*(\theta_m/\{C,D\}) \propto L^*(\{C,D\}/\theta_m)\pi^*(\theta_m) \tag{2.6}$$

where the constant of proportionality is given by $\int_\Theta L^*(\{C,D\}/u)\pi^*(du)$, (Θ, π^*) is the parameter space and π^* is a joint prior distribution of θ_m conditional to $\{c^*, d^*, \theta_e\}$. We consider now following marginal prior conditional distributions:

$$\left\{ \begin{array}{lcl} L^*(I_0/\theta_e) & = & \text{geom}(1-p_0) \\ L^*(\mu/I_0, \theta_e) & = & \text{beta}(1, (1-\kappa_1)/\kappa_1) \\ L^*(\gamma/I_0, \mu, \theta_e) & = & \text{beta}(1, (1-\kappa_3)/\kappa_3) \\ L^*(\beta/I_0, \mu, \gamma, \theta_e) & = & \text{beta}(1, (1-\kappa_2)/\kappa_2), \end{array} \right. \tag{2.7}$$

where:

$$p_0 = \begin{cases} R_p & \text{si} \quad R_p < 1 \\ \dfrac{\beta}{\beta + \delta(R_p - 1)} & \text{si} \quad R_p > 1 \\ 0.50 & \text{si} \quad R_p = 1, \end{cases} \tag{2.8}$$

geom$(1-p_0)$ denotes the geometric distribution with $1-p_0$ parameter(seasonal outbreaks start from in quasi-stationary regime[21]) and beta(a, b) is the beta distribution with shape parameters a and b, used to take into account outbreaks's characteristics and take a deviation from the uniform distribution generally used for these parameters with values in [0 , 1].

we recall that $R_p = \dfrac{n(1-p)\beta}{\delta(\mu + \delta + \gamma)}$ and κ_1, κ_2 and κ_3 are augmented data about the observations.

The data augmentation methods have often used to augment the observed data with the pieces of information required to write easily the likelihood [23], here the lethality rate(LR) for κ_1, the attack rate (AR) for κ_2 and $\kappa_3 = (1-\kappa_1)(1-\delta)$. Then we can write $\pi^*(\theta_m) =$

$$L^*(\beta/I_0, \mu, \gamma, \theta_e)L^*(\gamma/I_0, \mu, \theta_e)L^*(\mu/I_0, \theta_e)L(I_0/\theta_e) \tag{2.9}$$

We model the temporal evolution of an epidemic as a Poisson flow of infections with a binomial chain of deaths[24, 25]. Precisely we set:

$$L^*(C_{k+1}, D_{k+1}/C_k, D_k, \theta_m) =$$

$$L^*(D_{k+1}/C_{k+1}, C_k, D_k, \theta_m)\, L^*(C_{k+1}/C_k, D_k, \theta_m)$$

and

$$\begin{aligned} L^*(C_{k+1}/C_k, D_k, \theta_m) &= \text{Poiss}\left(\beta S_k I_k\right) \\ &\approx \text{Binom}\left(S_k, 1 - e^{-\beta I_k}\right) \end{aligned} \tag{2.10}$$

$$L^*(D_{k+1}/C_{k+1}, C_k, D_k, \theta_m) = \text{Binom}\left(C_{k+1}, \mu\right). \tag{2.11}$$

It follows from equations 2.10 and 2.11 that the complete data likelihood for our model is

$L^*(\{C, D\}/\theta_m) =$

$$\prod_{k=0}^{N-1} L^*(C_{k+1}/C_k, D_k, \theta_m)L^*(D_{k+1}/C_{k+1}, C_k, D_k, \theta_m). \tag{2.12}$$

3 Results and discussion

In this section, we present the results from the application of Metropolis-Hasting algorithm to related data collected from MDO Niger. Then, numerical simulations of the proposed model allows discussion about differentiation between regions with respect to the threat of measles outbreak.

3.1 Results

Using data of table 1, we estimate the vector parameters θ_m by Metropolis-Hasting MCMC sampling, the proposal density is a random walk chain. It is well know that rejection sampling takes a long time computationally, so we performed $100,000$ iterations to constitute a sample from the posterior distribution. The first $10,000$ iterations were discarded as the burn-in period. We aggregate our results in the following table 2.

Regions	I_0	γ	μ	β	R_p
Agadez	110	$0,49$	$0,00283$	$4,054 \times 10^{-5}$	$4,51$
Diffa	66	$0,61$	$0,00253$	$5,516 \times 10^{-5}$	$2,76$
Dosso	31	$0,73$	$0,00346$	$2,124 \times 10^{-5}$	$2,00$
Maradi	119	$0,67$	$0,00168$	$0,814 \times 10^{-5}$	$2,22$
Niamey	86	$0,61$	$0,00191$	$1,810 \times 10^{-5}$	$3,85$
Tahoua	163	$0,64$	$0,01472$	$0,989 \times 10^{-5}$	$3,42$
Tillabery	71	$0,64$	$0,00693$	$1,053 \times 10^{-5}$	$1,80$
Zinder	576	$0,67$	$0,00165$	$1,390 \times 10^{-5}$	$2,75$

Table 2: Estimated parameters measles epidemics 2018 in Niger regions

It follows from these data that Tahoua and Zinder regions are the most affected, followed by the Agadez region. These regions remain potentially vulnerable with the highest R_p values for years to come. The Maradi region, between two high-risk regions, is not spared from the threat. In Niamey region, as well as in that Agadez region, measles epidemic is likely to spread very quickly, if the response is not immediate, because the R_p value is relatively high and the vaccination coverage value small in these regions. But these regions, as well as Diffa and Tillabery regions, are less affected by epidemics, due to their low birth rates.

Figure 8 shows distribution of estimates of R_p and reported cases 2018 in Niger regions taken from MDO database. The shading intensity reflects high levels of reported cases in indicated regions, e.g. Maradi, Tahoua and Zinder.

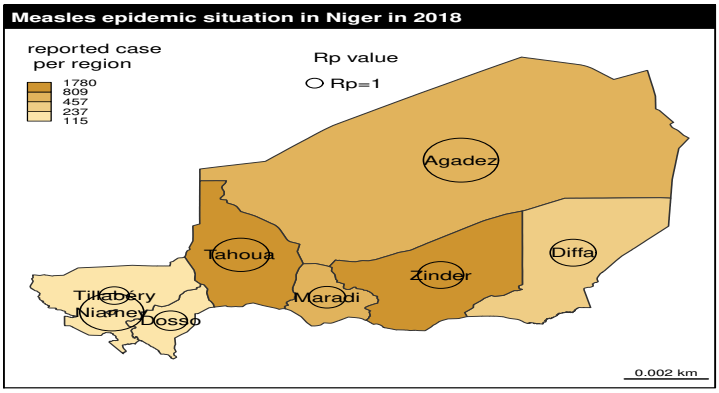

Figure 8: Distribution of R_p circles areas give magnitude of R_p

MCMC algorithn convergences are plotted in figures 9 to 12 for each region. Convergences were visually assessed.

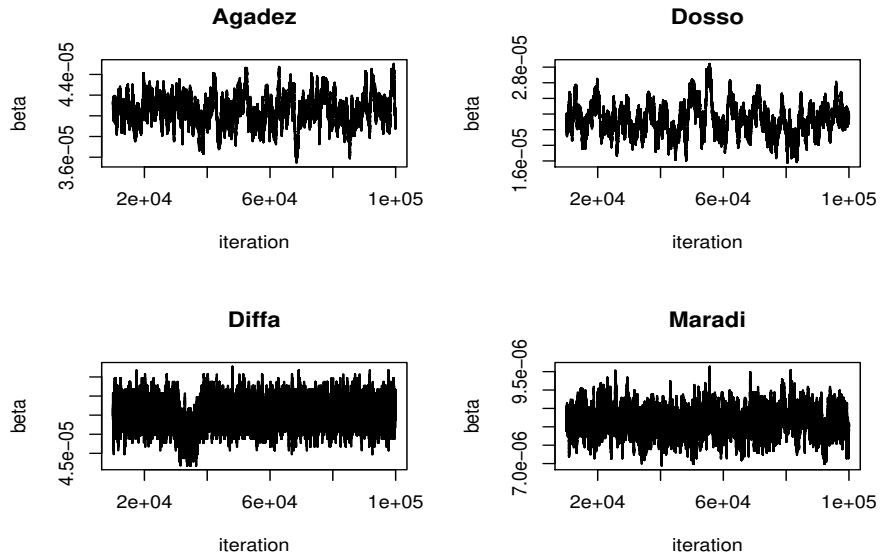

Figure 9: Markov chain convergence for β: 100 000 iterations estimated values: Agadez : $4,054 \times 10^{-5}$, Diffa : $5,516 \times 10^{-5}$, Dosso : $2,124 \times 10^{-5}$, Maradi : $0,814 \times 10^{-5}$

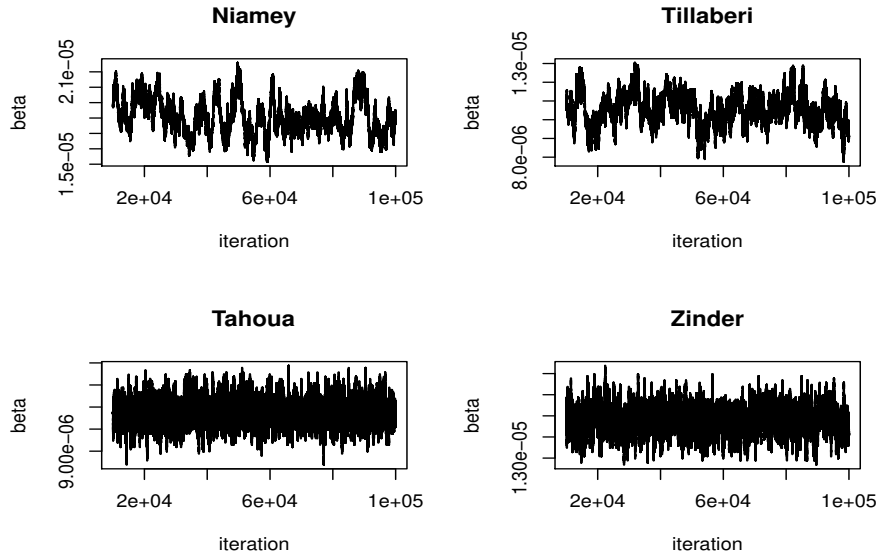

Figure 10: Markov chain convergence for β: 100 000 iterations estimated values: Niamey : $1,810 \times 10^{-5}$, Tahoua : $0,989 \times 10^{-5}$, Tillaberi : $1,053 \times 10^{-5}$, Zinder : $1,390 \times 10^{-5}$

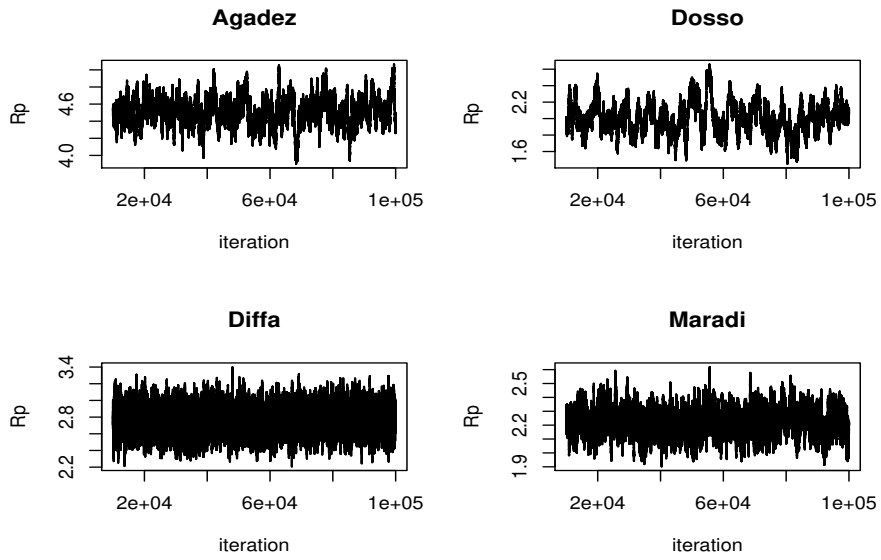

Figure 11: Markov chain convergence for R_p: 100 000 iterations
estimated values: Agadez : $4,51$, Diffa : $2,76$, Dosso : $2,00$, Maradi : $2,22$

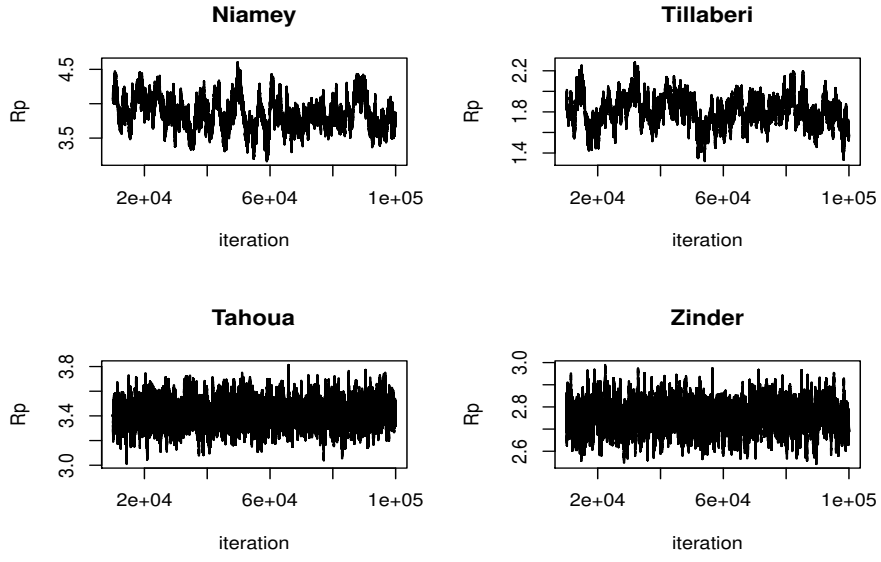

Figure 12: Markov chain convergence for R_p: 100 000 iterations
estimated values: Niamey : $3,85$, Tahoua : $3,42$, Tillaberi : $1,80$, Zinder : $2,75$

3.2 Simulations

For the simulation, we used marginal distributions of $(C_k)_{1\leq k\leq 26}$ and $(D_k)_{1\leq k\leq 26}$, defined in equations 2.10 and 2.11, given parameters $\theta_m = (I_0, \beta, \mu, \gamma)$ and $\theta_e = (S_0, \delta, n, p)$ with estimated values. Here, C_k is the number of new infections occurring during the time period $]k-1; k[$, not to be confused with I_k, the number of infected at time k.

The process $(C_k)_{1\leq k\leq 26}$ (biweekly cases) is perturbed both by the report rate ρ and health services response to the epidemic, to give reported cases. See figures 13 et 14, two samples paths of simulated cases (in blue and red), reported cases 2018 (solid line) and simulated cases means.

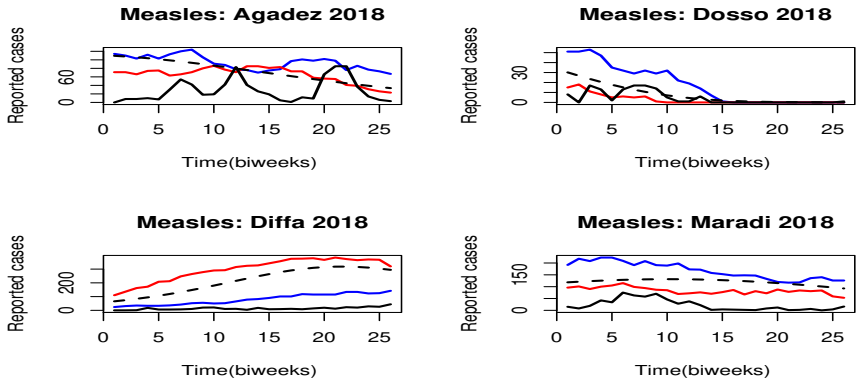

Figure 13: Tendency measles epidemic 2018

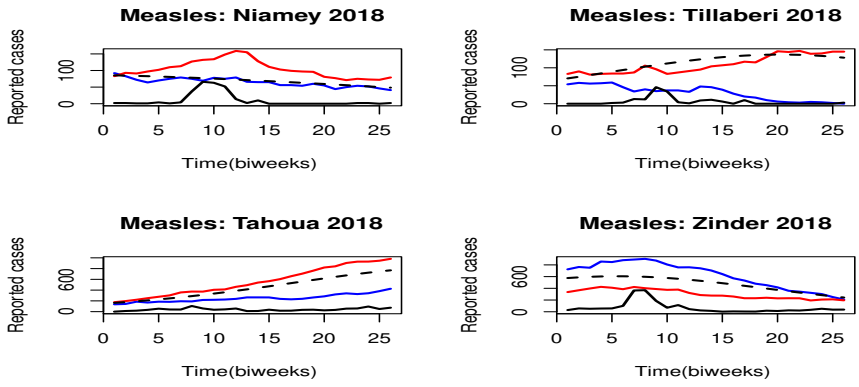

Figure 14: Tendency measles epidemic 2018

3.3 Discussion

In Niger, Measles incidence presents a seasonal cycle with a period varying from 1 to 3 years and increased incidence coinciding with the dry season [7, 8, 9].

Mathematical models allow a better understanding of the dynamics of disease spread in a population. However, these models depend on many parameters, which often limits their range in statistical analysis of epidemic spread. Among them, we can quote difficulty in data collection processes, estimation of statistics parameters, estimation of the correlation between random parameters, numerical resolution of partial differential equations or stochastic differential equations, with a natural problem of discretization of functions, etc.

Our results should start a discussion and could aid the stakeholders to design strategic vaccination coverage for each region in Niger. In such a process, it is very important to explain the transmission coefficient of the disease and the effective reproduction number. We suggest to consider the vaccination coverage (VC), the vulnerable age group, and the number of cases reported in the 8 regions. Under this scheme, only the vaccination coverage variable seems to explain better these two parameters, as shown in figure 15. Here, we refer to the dots Az for Agadez region, Da for Diffa region, Do for Dosso region, Mi for Maradi region, Ta for Tahoua Region, Ty for Tillabery region and Zr for Zinder region.

It appears that Tahoua, Maradi, Tillaberi, and Diffa regions show a large trend. Meanwhile, the last two regions remain less threatened due to the low value of R_p in these regions.

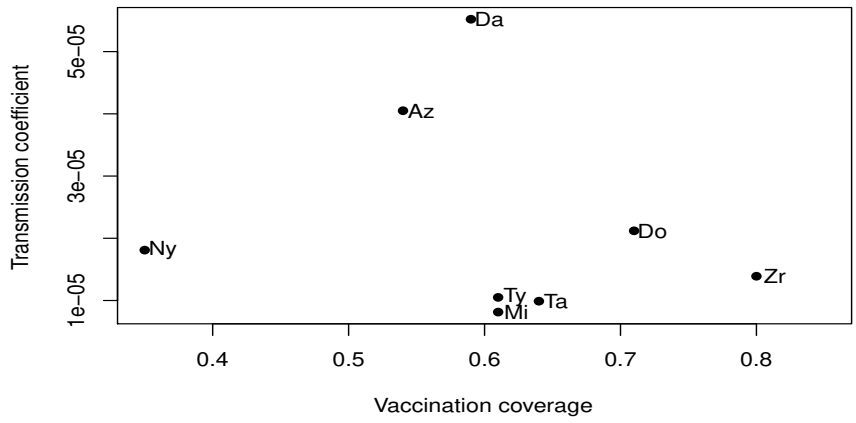

Figure 15: VC compared with transmission coefficient

4 Conclusion

Measles epidemics are less recurrent in regions with low birth rates such as Dosso and Diffa regions, except for Niamey region, which has a high rate of seasonal migration. Measles remains endemic in Niamey, Tahoua, Tillabery, and Zinder regions, despite a fairly high vaccination coverage in these regions. Three essential factors have been noted in the emergence of epidemics in these regions: seasonal migration which may concern the age group from 0 to 15 years old, low vaccination coverage, and the relatively high birth rate for regions with low vaccination coverage.

We note here the important role of demographic parameters and response strategies in the spread of an epidemic. Outbreak response services need to take this into account to enhance prompt reactive intervention toward morbidity reduction. The target vaccination coverage given by the WHO is 95% to prevent the population against the spread of measles. At the national level, only 68.7% of children receive the measles vaccination before they turned 1-year-old [14]. Coming to the full vaccination coverage, it was estimated at 52.0% with 4.1% of children having never received any vaccination [26].

Our work in this paper is restricted to a closed population, but we are in the process of extending it, to take immigration into account and see its impact on measles outbreaks in certain border regions of the country where the migratory flow is significant. Indeed, these regions(like Agadez, Tahoua, Zinder, Tillabery) which are refugee camps seem to be very vulnerable to measles outbreaks. The WHO recommendations suggest that vaccination interventions should be concentrated in closed high-risk populations such as refugee camps or schools [27].

References

[1] Bartlett T. "The molecular biology of the morbillivirus (measles) group,". Biochemical Society Symposium, vol. 53:pp. 25–37, 1987.

[2] WHO. "Fact about Measles,", Oct 2019. https://www.who.int/news-room/fact-sheets/detail, (accessed 11 juillet 2020).

[3] Kitengeso R. E. et al. "A Mathematical Model for Control and Elimination of the Transmission Dynamics of Measles.". Applied and Computational Mathematics, vol. 4,(6):pp. 396–408, 2015.

[4] Alkassoum S. et al. "Surveillance épidémiologique de la rougeole au Niger: Analyse de la base de données des maladies à déclaration obligatoire (mdo) de 2003 à 2015,". International Journal of Innovation and Scientific Research, vol. 17, no. 2:pp. 264–274, 2016.

[5] Mitku S. N. , Koya P. R. "Mathematical Modeling and Simulation Study for the Control and Transmission Dynamics of Measles,". American Journal of Applied Mathematics, vol. 5, no. 4:pp. 99–107, 2017.

[6] Moussa Tessa O. "Mathematical model for control of measles by vaccination,". In Proceedings of MSAS 06 Conference, MSAS Bamako Mali, August 2006, pp. 31-36.

[7] Blake A. , DJibo A. , Guindo O. , Bharti N. "Investigating persistent measles dynamics in Niger and associations with rainfall,". J. R. Soc Interface, vol. 17: 20200480:pp. 1–10, 2020. https://doi.org/10.1098/rsif.2020.0480.

[8] Moss W. J. "Measles,". The Lancet, vol. 390:pp. 2490–2502, 2017. https://doi.org/10.1016/S0140-6736(17)31463-0.

[9] Moss W. J. "Measles still has a devasting impact in unvaccinated populations,". PLoS Med., vol. e24, no. 4:pp. 0009–0010, 2007. https://doi.org/10.1371/journal.pmed.0040024.

[10] Hethcote H. W. "The Mathematics of Infectious Diseases,". SIAM Review, vol. 42, no. 4:pp. 599–653, 2000. https://doi.org/10.1137/S0036144500371907.

[11] Van der Driessche P. , Watmough J. "Reproduction numbers and sub-threshold endemic equilibria for compartmental models of disease transmission,". Mathematical Biosciences, vol. 180, Issues 1-2:pp. 29–48, 2002. https://doi.org/10.1016/S0025-5564(02)00108-6.

[12] Anderson R. M. , May R. M. "Infectious diseases of humans: dynamics and control,". Oxford University Press, Oxford, UK, 1991.

[13] MSP. "Annuaire des statistiques sanitaires du Niger,", 2019. http://www.snis.cermes.net.

[14] ICF , INS. "Enquête Démographique et de Santé et à Indicateurs Multiples du Niger 2012,", 2013. https://dhsprogram.com/pubs/pdf/fr277/fr277.pdf,(accessed 06 Dec. 2022).

[15] MDO–DSRE Niger. "Maladies à Déclaration Obligatoire – MDO de 2018,", 2018. https://www.who.int/news-room/fact-sheets/detail/measles,(accessed 11. Oct. 2019).

[16] Finkenstädt B. F. "A stochastic model for extinction and recurrence of epidemics estimation and inference for measles outbreaks,". Biostatistics, vol. 3, no. 4:pp. 493–510, 2002. https://doi.org/10.1093/biostatistics/3.4.493.

[17] Anderson R. M. , Rhodes C. J. "Power laws governing epidemics in isolated populations,". Nature, vol. 381:pp. 600–602, 1996. https://doi.org/10.1038/381600a0.

[18] Anderson R. M. , Jensen H. J. , Rhodes C. J. "On the critical behavior of simple epidemics,". Proceedings of the Royal Society of London, vol. B 264:pp. 1639–1646, 1997. https://doi.org/10.1098/rspb.1997.0228.

[19] Cliff A. D. , Haggett P. , Smallman-Raynor M. "Mesales: an historical geography of a major human viral disease from global expansion to local retreat,". Blackwell, Oxford, UK, vol. 19, Issues 4:pp. 1840–1990, 1993. https://doi.org/10.1177/030913259501900413.

[20] Seydou M. , Moussa Tessa O. "A Stochastic SVIR Model for Measles,". Applied Mathematics, vol. 12:pp. 209–223, March 2021. https://doi.org/10.4236/am.2021.123013.

[21] Seydou M. , Moussa Tessa O. "Approximations of Quasi-Stationary Distributions of the Stochastic SVIR Model for the Measles,". Applied Mathematics and Physics, vol. 9:pp. 2277–2289, September 2021. https://doi.org/10.4236/jam.2021.99145.

[22] Black F. L. "Measles,". In Viral Infections of Humans: Epidemiology and control, 1984.

[23] Cauchemez S. , Ferguson N. M. "Likelihood-based estimation of continuous-time epidemic models from time-series data: application to measles transmission in London,". J. R. Soc. Interface, vol. 5, no. 25:pp. 885–897, September 2008. https://doi.org/10.1098/rsif.2007.1292.

[24] M. J. , Bjørnstad O. N. , Dobson A. P. Ferrari. "Estimation and inference for R0 of an infectious pathogen by a removal method.". Math. Biosci., 198:pp. 14–26, October 2005. https://doi:10.1016/j.mbs.2005.08.002.

[25] Grais R. F. , Ferrari M. J. , Dubray C. , Bjørnstad O. N. , Grenfell B. T. "Estimating transmission intensity for a measles epidemic in Niamey, Niger: lessons for intervention.". Trans. R. Soc. Trop. Med. Hyg., 100:pp. 867–873, October 2005. https://doi:10.1016/j.trstmh.2005.10.014.

[26] Kunieda M. K. , Manzo M. L. , Shibanuma A. , Jimba M. "Rapidly modifiable factors associated with full vaccination status among children in Niamey, Niger: A cross-sectional, random cluster household survey,". PloS one, vol. 16, no. 3:pp. 1–12, March 2021. https://doi.org/10.1371/journal.pone.0249026.

[27] WHO. "Measles: Immunization, Vaccines and Biologicals,", August 2019. https://www.who.int/immunization/newsroom/new-measles-data-august-2019/en/, (accessed 20. Dec. 2019).